OPTIMAL FILTERING OF SENSOR SIGNALS FOR TAKE-OFF PERFORMANCE MONITORS (TOPM)

R. Khatwa
Department of Aerospace Engineering
University of Bristol
England

Abstract

Both pilot opinion and the accident statistics indicate a need to improve safety in the take-off phase. A major problem encountered is the high speed overrun of the runway during a rejected take-off (RTO). At present cockpit instrumentation which presents the type of information necessary for accurate performance during take-off is limited to the airspeed indicator. Additional information to monitor the progress of the take-off would warn pilots of any shortcomings and thus a take-off could be rejected at an earlier stage during the ground roll to prevent a high speed overrun. This paper reviews the development of an efficient Take-Off Performance Monitor (TOPM) and focuses on the role of the Kalman filter in deducing optimal estimates of the take-off conditions. The goal of achieving a high level of accuracy in the outputs while also employing filter algorithms that are both stable and robust has been achieved. Important improvements in operational safety could result form the widespread use of efficient take-off monitors.

Nomenclature

b_a	accelerometer bias	m/s^2
b_g	GSS bias	m/s
b_α	gyroscope drift-rate bias	rad/s
$\mathbf{F}$	$n \times n$ continuous system dynamics matrix	
$\mathbf{G}$	$n \times r$ plant noise input matrix	
g	acceleration due to gravity	m/s^2
$\mathbf{H}$	$m \times n$ measurement matrix	
$\mathbf{K}$	$n \times m$ Kalman gain matrix	
$\mathbf{P}$	$n \times n$ covariance matrix of $\hat{\underline{x}}$	
$\mathbf{P}'$	$n \times n$ covariance matrix of $\underline{x}'$	
$\mathbf{Q}$	$r \times r$ system noise covariance matrix	
$\mathbf{R}$	$m \times m$ measurement noise covariance matrix	
R_e	Earth equatorial radius	m
$\mathbf{S}$	$n \times n$ square root of $\mathbf{P}$	
$\mathbf{S}'$	$n \times n$ square root of $\mathbf{P}'$	
t	time	s
$\mathbf{U}$	$r \times r$ square root of $\mathbf{Q}$	
u	IRS velocity in North direction	m/s
$\mathbf{V}$	$m \times m$ square root of $\mathbf{R}$	
$\underline{v}$	m-dimensional Gaussian measurement noise vector	
v	IRS velocity in East direction	m/s
V_g	GSS velocity in runway along-track direction	m/s
$\underline{w}$	r-dimensional Gaussian plant noise vector	
w	IRS velocity in vertical direction	m/s
w_a	accelerometer white Gaussian noise	m/s^2
w_g	GSS white Gaussian noise	m/s
w_α	gyroscope drift-rate white Gaussian noise	rad/s
$\underline{x}$	n-dimensional state vector	
$\underline{z}$	m-dimensional measurement vector	
Δt	sampling interval	s
Δu	North direction velocity error	m/s
ΔV	error measurement	m/s
ΔV_g	error in GSS signal	m/s
Δx	North direction distance error	m
$\Delta\Theta$	tilt error in East platform stabilising gyroscope	rad
δ_{kl}	Kronecker delta function	
ε	statistical expectation	
Φ	$n \times n$ discrete system state transition matrix	
Γ	$n \times r$ system noise coefficient matrix	
σ^2	variance of noise process	
Θ	platform rotation about East axis	rad
θ_R	runway heading	rad

Subscripts

LO	lift off
M	measured parameter
R	rotation
1	decision
2	denotes take-off safety speed

Dressings

.	time derivative
'	time update
^	optimal estimate

1. Introduction

In January 1982, an Air Florida Boeing 737 attempting to leave Washington National Airport was unable to climb properly due to sub-standard thrust development throughout its ground roll. The aircraft crashed into a bridge with loss of 78 lives. The accident investigation found that there was significant wing contamination by ice, thus affecting the engine inlet pressure probes. Before take-off roll commenced the pilot attempted to set take-off thrust using Engine Pressure Ratio, but his adjustment to an indicated value of 2.04 produced an effective value of 1.70 due to the pressure probe blockage. Consequently a lower-than-normal level of thrust was applied during take-off.

The ensuing accident report recommended the development of a TOPM, as existing airworthiness requirements contained several inadequacies. The accelerate-stop performance and thus the field length computations are based on the assumption that the aircraft acceleration will be normal up to the decision speed (V_1). Currently, the scheduled accelerate-stop distance may be exceeded even before the decision point is reached and a decision made to reject take-off. On any day, factors such as runway contamination, degraded engine performance, actual runway profile (as opposed to 'effective gradient') and tyre failures can adversely affect the airplane acceleration and cannot therefore be accounted for during standard certification procedures . Furthermore, for aircraft certified in accordance with US Federal Aviation

Regulations (FAR), the decision speed and field length calculations for contaminated surface operations are based on a clean, dry runway. Thus the accelerate-stop criteria cannot always be guaranteed to provide an acceptable level of safety in real situations.

Accident data compiled by the Society of Automotive Engineers[1] (SAE) indicates very clearly that the take-off accident rate has not declined during the last two decades. Service history indicates that most fatal accidents are due to some form of performance deficiency and that catastrophic overruns continue to occur even when the take-off is rejected at speeds substantially below V_1. Between 1962 and 1978 over 25% of the overruns[2] occurred due to RTOs initiated at a speed equal to or below V_1. Pilot opinion sought during this study revealed that common feelings of anxiety existed among air crew about the thoroughness and accuracy of take-off communications and decisions. It was made eminently clear that the take-off decisions and accelerate-stop problems deserved scrutiny.

It is clear that during the take-off roll the pilot currently has no means except his instinct by which to determine whether the performance is normal for the existing weight and engine setting. Thus in order to improve safety in this area much more comprehensive monitoring of the take-off is required. An efficient TOPM would assist the pilot in keeping the progress of the take-off constantly in view, so as to make it easier to decide if a take-off can safely be continued or to support the decision to abandon it, even before he reaches V_1. There is little doubt that the predictive capacity of a TOPM is crucial to flight safety if only because warning would be given before a critical situation occurred. Consideration has been given to both distance-to-go runway markers and time-to-speed checks in the past, but both have been discarded as insufficient for safe civil operations. Despite the recommendation noted in 1982, only limited progress has been made in producing a reliable system. In contrast to work reported to date, which considers only a deterministic approach, this paper reviews the development of an efficient TOPM and focuses on the processes required to deduce optimal estimates of the take-off conditions by employing Kalman filtering techniques.

The remainder of this paper is sub-divided as follows. Section 2 examines the possible benefits of a take-off monitor and outlines the main problems that must be tackled for the successful development of a take-off monitor. The equations for the Kalman formulation of a statistical filter are then summarised in Section 3. The implementation of the filter is illustrated by application of the equations to a simple example. Next, simulation results are presented for a typical take-off using an Inertial Reference System (IRS) aided by an independent groundspeed signal. Finally, support is provided for the attitude that an efficient system of this kind would contribute significantly to air safety.

2.0 General Principles for a Display

Fundamental to the objectives of this research is the desire to produce a display with reliable predictive capacities which will provide warnings of take-off dangers earlier than would otherwise be the case. Numerical integration of the set of equations, to which the filter outputs contribute values of sensed parameters, will provide at least

(a) the current position of the aircraft on the runway (l_c), a continually lengthening bar growing within a simple runway outline,
(b) stopping distance required for current speed (S_c),
(c) the predicted position which the aircraft will reach when its speed becomes V_1 (l_{v1}) or V_R, (this could be represented by a narrow bar across the runway strip, and preferably coloured (green) and visible as the 'next marker' along the strip)
(d) the predicted stopping distance required for the aircraft when it reaches V_1 (S_{v1}). (This would be represented by another narrow bar (red) and initially visible as another marker beyond the 'next marker'.)

A simple form of the display would be as shown in Fig.1.

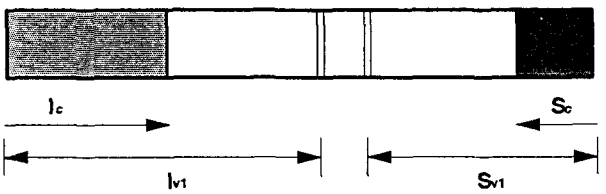

Fig. 1 Simple TOPM Display

Indeed these positions would be calculated and displayed using nominal payload data along with other nominally correct data such as engine thrust, while taxiing out. Thus those take-offs that were only marginally safe would become apparent at that stage.

After brake-release, these critical lengths would be displayed on the basis of real measured data and 'forward computations'. The rolling resistance characteristics of the runway need to be established, including runway or tyre resistance and impingement drag associated with runway contaminants whether dirt or snow. Runway contaminants will affect braked wheels and friction coefficients cannot be assumed to remain unchanged for stopping performance predictions. The TOPM algorithms will need to take into account the extent of engine or tyre failures and the consequential effect on the aircraft's performance. Other anomalies such as excess weight unknown to the pilot must also be reflected in all performance computations to avoid misleading the crew. The current windspeed as obtained from an onboard windspeed estimator should be incorporated in all predictions such that dangerous situations arising from unexpected wind changes are prevented. The accuracy of the prediction phase would be enhanced if the actual runway profile rather than the official effective gradient were employed.

All four variables will be re-evaluated regularly, subject to data being collected from[3]

- Inertial Reference System (accelerometers and gyroscopes)
- Air Data Computer (ADC) (wind/velocity sensors)
- Groundspeed sensor (GSS) (eg. wheel rotation rate or doppler)
- Wheel Monitors (eg. Tyre Pressure Indicating System to monitor 'tyre health')
- Engine parameters in order to measure gross thrust and thus monitor engine health[4]
- An algorithm that estimates the effective runway rolling friction coefficient

and any important consequences of changes in these data would be displayed as frequently as the chosen screen-refresh rate.

The following could happen, with consequences noted:

- Some loss of thrust: l_{V1} would be extended, but other lengths would be unaffected (assuming that credit was not given for reverse thrust when predicting stopping performance).
- Multiple tyre failure: l_{V1}, S_{V1} and S_c would all be lengthened.

As the two bars associated with l_{V1} and S_{V1} close upon each other, the pilot's margin for error, delay or decision narrows and if the order of the two bars is reversed, ie. the pilot sees the red bar as the 'next marker' along the runway strip, he can forsee problems before they arise. Take-off can be aborted before a threat to safety arises.

2.1 The Runway Requirement after Decision Speed

The description above embodies the central predictive concept, but is probably short on realism. The proper requirements will have to take account of the following, namely the distances associated with stopping, or clearing the screen height, from the runway position at which a decision is made.

Fig. 2 shows the layout of speeds and positions relative to the clearance required at the screen. The allowable stopway length is also shown beyond the formal runway limit. Three speeds are assumed to exist in ascending order along the runway at successively greater distances from brake-release, namely V_1, V_R and V_{LO}. There follows the flare and eventual clearance as required, reaching V_2.

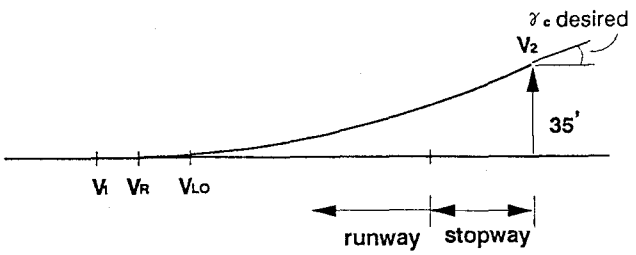

Fig. 2 Take-Off Reference Speeds

For the TOPM there is a need to calculate the total length beyond a critical speed (V_1 or V_R) to clear the screen and to achieve an agreed V_2 based on current aircraft data, eg. all-up-weight, for the climb performance required. The total distance required would involve a calculation backwards from the screen height effectively. It is this length which really governs the 'go/no go' decision.

2.2 A More Realistic Display Requirement

The description in 2.0 above is useful for considering concepts of prediction and warning, but is less than realistic for a particular runway. The important requirements for a decision to support a safe take-off or abort might be met by the following variation.

Fig. 3 shows a comparable display which assumes that the aircraft joins the runway at some point near a taxiway and removed from the near end of the runway.

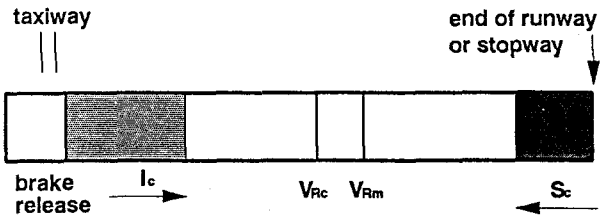

Fig.3 Realistic TOPM Display

Details of the runway could be entered into the TOPM manually, but in a mature system they would probably be stored in much the same way that current navigation data are held in memory and would include facts such as

- runway profile data
- length, taxiway junctions, stopway provision
- runway heading
- special obstructions to be cleared
- nominal runway friction data, if available.

The operation of the display and supporting computations would be the same as in 2.0 above but the two bars shown in Fig. 3 would be defined as follows:

(a) V_{Rc} is the position along the runway at which a critical speed, say V_R, will be reached and indicating that the take-off 'can go'.
(b) V_{Rm} is the position on the runway, calculated backwards from the screen or stopway, at which the same critical speed must be reached in order to satisfy the minimum safe take-off requirements and at which the take-off 'must go'.

The relative positions of the two warning bars 'can go' and 'must go' will provide the predictive assistance to the pilot. These bars would migrate if the take-off parameters (eg. engine health, tyre conditions, runway contamination) changed during the ground roll and the pilot would get earlier than normal warning that a difficult situation was impending.

The capacity to detect a significant performance deficiency can be enhanced by employing a simple acceleration monitor, which essentially distinguishes between 'acceptable' and 'unacceptable' acceleration. The danger with this form of monitoring is that some take-offs could be rated visually as sub-normal while the performance would still be within acceptable limits for the current runway. An efficient acceleration monitor has the ability to discriminate properly between safe and unsafe situations in order to avoid a high rate of unnecessary RTOs. The acceptable level of acceleration for performance assessment purposes must be deduced.

Inherent in the outputs of a TOPM are errors associated with both the hardware and software which may adversely affect the safety of the take-off. For example, uncertainties introduced into the stopping distance prediction would display to the pilot a distance that was either overestimated or one that was

underestimated. Hardware errors will be introduced into the TOPM outputs as there will always be uncertainty in the sensor outputs, even after the filtering process. Analysis must show that the possibilities of 'failure to warn' and 'nuisance to warn' are kept to an absolute minimum in order to avoid a high rate of unnecessary RTOs and to insure that the display gives adequate warning of an approaching emergency.

2.3 The Definition of Sufficient Warning

Fig. 4 shows the usual method of finding a balanced field length and defining V_1, the decision speed which allows

(a) continued take-off with a failed engine and clearance to the screen height at V_2
(b) emergency stop within the length that includes remaining runway and the stopway.

By definition, the balanced field length has the two lengths for (a) and (b) equal, implying that the fictitious screen is at the end of the the stopway. Both the 'go' and the 'no go' criteria demand the same length to complete the operation.

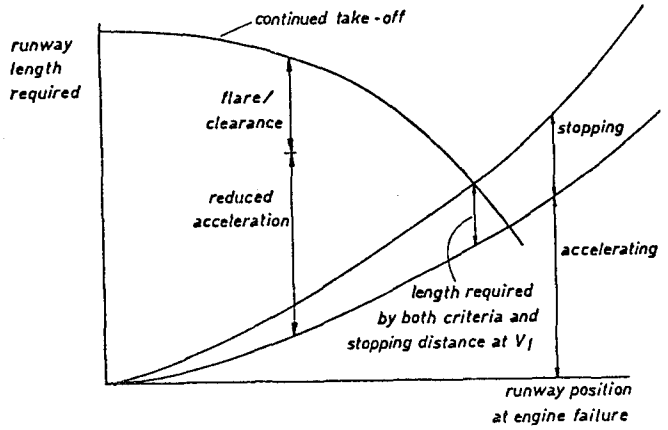

Fig. 4 Balanced Field Length Concept

The equivalence of the two lengths assumes that stopping distance has been calculated with valid friction data. These could change and it can be argued that instead of a reverse calculation of the length given in Fig. 2, from V_2, a comparable reverse calculation should be made from the end of the stopway, to find the requirement for runway remaining at the latest decision point. Whichever criterion is used, there can be displayed a 'must go' position on the runway strip and, for convenience, only one such position is shown on Fig. 3 namely V_{Rm}.

3.0 Optimal Filtering of Inertial Flight Data

The objective of this section is to propose a suitable state estimator which filters the data from two independent sources to deduce optimal estimates of the take-off conditions. Work reported to date considers only a deterministic approach to filter these signals. For example, a fixed-gain second-order Complementary filter has been utilised in a recent system[5]. The Kalman filter approach to deduce optimal estimates of the errors present in the measurement signals is investigated here.

3.1 Data Sources

A method of measuring aircraft motion needs to be employed so that the instantaneous aircraft performance is known and to enable a prediction of future performance. Whilst conventional sources of data such as the IRS and ADC are bound to be used, there is also a need to employ alternative sources such as rotation servos in the wheel units and perhaps a reflective method such as forward-looking doppler or a mechanism akin to a radio altimeter directed toward highly reflective targets at each runway threshold. It is recognised that the selection of sensors normally available onboard would depend upon the aircraft in question eg. Transport, General Aviation. A mathematical model of a Boeing 747 aircraft has been employed in this investigation which houses both an IRS and an alternative GSS to determine airplane velocity and position on the runway.

The IRS consists of accelerometers for measuring specific forces acting on the aircraft, plus a stabilised platform containing rate gyros for measuring aircraft attitude and attitude rates. The IRS considered herein employs the geographic axes (ie. East, North and vertical) as the reference frame for measurements and we assume that the platform is not aligned correctly with the geographic axes due to an initial tilt error and gyro drift. The East, North and vertical platform stabilising gyroscopes are in error by angles $\Delta\Theta$, $\Delta\varphi$ and $\Delta\beta$ respectively. It is assumed that the GSS provides measurements in the runway reference frame.

The data from all motion sensors must be processed by filter algorithms in a common frame of reference. The roll, pitch and heading measurements, together with the known runway heading, are used to compute the appropriate transformation matrix between platform variables and the runway reference frame. This matrix can then be employed to convert measurements into their appropriate components in the required reference frame. The relationship between geographic, platform and runway axes is illustrated below.

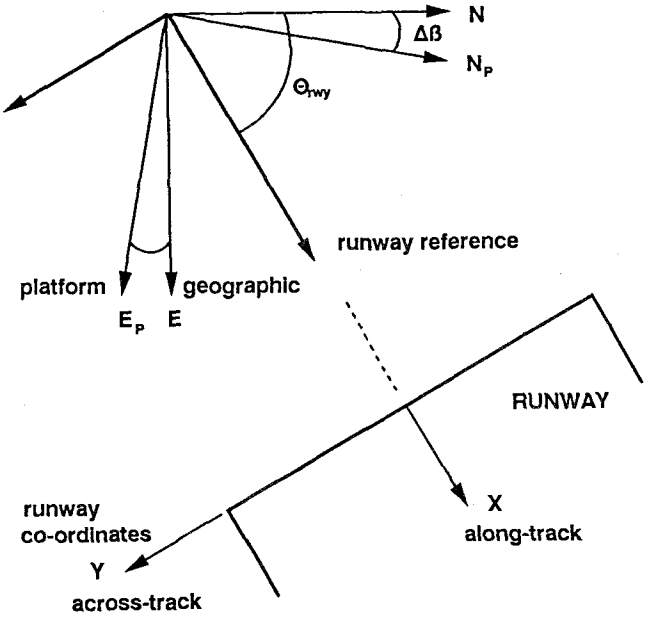

Fig. 5 Co-ordinate Systems

For this investigation it has been assumed that the runway along-track direction is aligned with geographic North and the aircraft is constrained to move along a meridian of a non-rotating Earth. The IRS will then indicate directly the acceleration along the runway and the East velocity is taken to be zero. In addition, the angle of latitude can be assumed to remain constant during the take-off manoeuvre.

3.2 Kalman Filter Algorithm

The mathematical model of the plant used in the Kalman filter is assumed to be a Markov process defined by the following difference equation

$$\underline{x}(k+1) = \Phi(k+1,k)\underline{x}(k) + \Gamma(k)\underline{w}(k) \qquad (1)$$

where $\underline{x}(k)$ is the n-dimensional state vector, Φ is the $n \times n$ nonsingular state transition matrix, Γ is the $n \times r$ system noise coefficient matrix and $\underline{w}(k)$ is an r-dimensional process noise vector. It is assumed that the measurements are a linear function of the system states and thus the discrete observations are given by

$$\underline{z}(k) = \mathbf{H}(k)\underline{x}(k) + \underline{v}(k) \qquad (2)$$

where $\underline{z}(k)$ is the m-dimensional measurement vector, $\underline{v}(k)$ is the $m \times 1$ measurement noise vector and $\mathbf{H}(k)$ is the $m \times n$ measurement matrix. Both $\underline{w}$ and $\underline{v}$ are assumed to be uncorrelated zero-mean Gaussian white-noise processes. The noise statistics are

$$\varepsilon\{\underline{w}(k)\} = 0 \qquad \varepsilon\{\underline{v}(k)\} = 0 \qquad \text{for all } k$$

$$\varepsilon\{\underline{w}(k)\underline{w}^T(l)\} = \mathbf{Q}(k)\delta_{kl}$$

$$\varepsilon\{\underline{v}(k)\underline{v}^T(l)\} = \mathbf{R}(k)\delta_{kl}, \qquad \mathbf{R}(k) > 0 \ .$$

Assume, also, that the state vector initial condition, $\underline{x}(0)$, is uncorrelated with respect to $\underline{w}$ and $\underline{v}$. The best estimate of the state, $\hat{\underline{x}}(k+1)$, and its variance, $\mathbf{P}(k+1)$, at time t_{k+1} can be updated for minimum variance by the following Kalman update equations[6].

Extrapolation between measurements

$$\underline{x}'(k+1) = \Phi(k+1,k)\hat{\underline{x}}(k) \qquad (3)$$

$$\mathbf{P}'(k+1) = \Phi(k+1,k)\mathbf{P}(k)\Phi^T(k+1,k) + \Gamma(k)\mathbf{Q}(k)\Gamma^T(k) \qquad (4)$$

Measurement update

$$\mathbf{K}(k+1) = \mathbf{P}'(k+1)\mathbf{H}^T(k+1)[\mathbf{H}(k+1)\mathbf{P}'(k+1)\mathbf{H}^T(k+1) + \mathbf{R}(k+1)]^{-1} \qquad (5)$$

$$\hat{\underline{x}}(k+1) = \underline{x}'(k+1) + \mathbf{K}(k+1)[\underline{z}(k+1) - \mathbf{H}(k+1)\underline{x}'(k+1)] \qquad (6)$$

$$\mathbf{P}(k+1) = \mathbf{P}'(k+1) - \mathbf{K}(k+1)\mathbf{H}(k+1)\mathbf{P}'(k+1) \qquad (7)$$

with initial conditions

$$\hat{\underline{x}}(0) = \varepsilon\{\underline{x}(0)\}$$

$$\mathbf{P}(0) = \varepsilon\{[\underline{x}(0)-\hat{\underline{x}}(0)][\underline{x}(0)-\hat{\underline{x}}(0)]^T\}$$

3.2.1 Square Root Formulations.

Under certain operating conditions it has been shown that the Kalman filter algorithm above can be unstable as the state estimation errors actually diverge with time[7]. The two common causes of filter divergence are inaccuracy in modelling the system, and round-off errors inherent in the implementation of the filter equations on a finite word-length digital computer. Modelling errors can be overcome by use of random forcing functions[6] which causes the more recent measurements to be weighted higher than past measurements. For the filter to operate successfully one important requirement is to propagate the covariance matrix $\mathbf{P}$ (and $\mathbf{P}'$) accurately as the elements of $\mathbf{P}$ decrease to very small values with time. In the presence of machine-caused errors the covariance matrix ceases to be positive definite and symmetric which are essential to a covariance matrix. The square root formulation of the conventional filter circumvents this difficulty by computing the square root of $\mathbf{P}$ instead of $\mathbf{P}$ and thereby cuts in half the number of significant figures required of the computer. This approach is therefore adopted in the proposed design.

The covariance square roots are defined as

$$\mathbf{P}'(k) = \mathbf{S}'(k)\mathbf{S}'^T(k) \qquad (8)$$

$$\mathbf{P}(k) = \mathbf{S}(k)\mathbf{S}^T(k) \qquad (9)$$

$$\mathbf{Q}(k) = \mathbf{U}(k)\mathbf{U}^T(k) \qquad (10)$$

and

$$\mathbf{R}(k) = \mathbf{V}(k)\mathbf{V}^T(k) \ . \qquad (11)$$

The time update of the covariance matrix is given by[7]

$$\mathbf{P}'(k+1) = [\Phi(k+1,k)\mathbf{S}(k) : \Gamma(k)\mathbf{U}(k)]\begin{bmatrix}\mathbf{S}^T(k)\Phi^T(k+1,k) \\ \mathbf{U}^T(k)\Gamma^T(k)\end{bmatrix} \qquad (12)$$

which may be verified by performing the multiplication on the right hand side of the equation and comparing the result with (4). The following two-step procedure is used to compute the square root $\mathbf{S}'^T(k+1)$:

$$\mathbf{A}^T = \begin{bmatrix}\mathbf{S}^T(k)\Phi^T(k+1,k) \\ \mathbf{U}^T(k)\Gamma^T(k)\end{bmatrix} \qquad (13)$$

and

$$\mathbf{S}'^T(k+1) = \mathbf{A}^T \qquad (14)$$

where $\mathbf{A}^T$ is reduced to upper triangular form by employing the modified Gram-Schmidt orthogonalisation[7] procedure.

The square root formulation for the measurement update of the covariance matrix due to Andrews[8] is

$$\mathbf{S}(k+1) = \mathbf{S}'(k+1)\{\mathbf{I} - \mathbf{Z}(\mathbf{W}^T)^{-1}(\mathbf{W} + \mathbf{V}(k+1))^{-1}\mathbf{Z}^T\} \qquad (15)$$

where

$$\mathbf{Z} = \mathbf{S}'^T(k+1)\mathbf{H}^T(k+1)$$

and

$$\mathbf{W}\mathbf{W}^T = \mathbf{R}(k+1) + \mathbf{Z}^T\mathbf{Z} \ . \qquad (16)$$

This procedure may be verified by multiplying (15) by its transpose and comparing the result with (7).

3.3 State Equations for the Kalman Filter

The 'indirect' approach is used in which the error states of the dynamic process are estimated as opposed to the actual physical states. The estimates are computed by differencing the basic navigation outputs as produced by the different systems and the resulting error measurements are then processed by the filter. These error states are used to correct the outputs of the navigation systems in a feedforward mechanisation in order to produce best estimates of the take-off conditions. This approach is illustrated below.

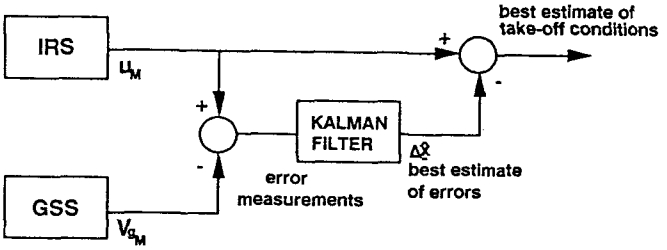

The statistical error models on which the filter is to be based must be reasonably complex if they are to describe the 'real world' accurately. In contrast, error models that are too complex may cause the storage and computation time constraints to be exceeded. Thus one of the basic design problems is to ensure a sensible balance between complexity and performance.

The error in a state is defined as the indicated value minus the true value. As an example, only simple models of the sensor uncertainties are used in this study. Typical IRS errors would be accelerometer biases, platform tilt errors, gyro drift and white Gaussian noise variables. The minor effects of gyro drift during take-off are included here for completeness but in practice a lower order error model would probably be employed. The tilt error introduces components of 'g' and vertical acceleration, $\dot{w}_M$, in the accelerometer measurement aligned with the North axis. The error equation for the North axis acceleration measurement is

$$\begin{aligned} \Delta\dot{u} &= \dot{u}_M - \dot{u} \\ &= \Delta\Theta(\dot{w}_M + g) + b_a + w_a \quad . \end{aligned} \tag{17}$$

It is assumed here that $\dot{w}_M$ can be measured with negligible error. As $\Delta\Theta$ is small, the effect of a measurement $\dot{w}_M$ corrupted with noise and biases will be negligible. The dynamic system generating the constant random variable b_a is of course

$$\dot{b_a} = 0 \quad . \tag{18}$$

The gyro drift-rate error model is assumed to consist of a bias component and a white noise process. The error equation for the drift rate is

$$\begin{aligned} \dot{\Delta\Theta} &= \dot{\Theta}_M - \dot{\Theta} \\ &= \left[-\frac{u_M}{R_e} + b_\alpha + w_\alpha \right] + \frac{u}{R_e} \\ &= -\frac{\Delta u}{R_e} + b_\alpha + w_\alpha \end{aligned} \tag{19}$$

and by definition

$$\begin{aligned} \dot{b_\alpha} &= 0 \\ \dot{\Delta x} &= \Delta u \quad . \end{aligned} \tag{20}$$

The error model assumed for the GSS measurement is defined as

$$\begin{aligned} \Delta V_g &= b_g + w_g \\ \dot{b_g} &= 0 \quad . \end{aligned} \tag{21}$$

The error measurement at discrete time intervals is

$$\Delta V = u_M - V_{g_M} = \Delta u - \Delta V_g \quad . \tag{22}$$

The differential equations for the error states may be written as

$$\dot{\underline{x}}(t) = F(t)\underline{x}(t) + G(t)\underline{w}(t) \tag{23}$$

and thus

$$\begin{bmatrix} \Delta\dot{u} \\ \Delta\dot{x} \\ \dot{\Delta\Theta} \\ \dot{b_a} \\ \dot{b_\alpha} \\ \dot{b_g} \end{bmatrix} = \begin{bmatrix} 0 & 0 & (g+\dot{w}_M) & 1 & 0 & 0 \\ 1 & 0 & 0 & 0 & 0 & 0 \\ -1/R_e & 0 & 0 & 0 & 1 & 0 \\ 0 & 0 & 0 & 0 & 0 & 0 \\ 0 & 0 & 0 & 0 & 0 & 0 \\ 0 & 0 & 0 & 0 & 0 & 0 \end{bmatrix} \begin{bmatrix} \Delta u \\ \Delta x \\ \Delta\Theta \\ b_a \\ b_\alpha \\ b_g \end{bmatrix}$$

$$+ \begin{bmatrix} 1 & 0 \\ 0 & 0 \\ 0 & 1 \\ 0 & 0 \\ 0 & 0 \\ 0 & 0 \end{bmatrix} \begin{bmatrix} w_a \\ w_\alpha \end{bmatrix} \quad . \tag{24}$$

The associated measurement equation is

$$\underline{z}(t) = H(t)\underline{x}(t) + \underline{v}(t) \tag{25}$$

or

$$\Delta V = [1\ 0\ 0\ 0\ 0\ -1] \begin{bmatrix} \Delta u \\ \Delta x \\ \Delta\Theta \\ b_a \\ b_\alpha \\ b_g \end{bmatrix} - w_g \quad . \tag{26}$$

Formulating the Kalman filter for implementation on a digital computer requires the continuous state space model defined above to be converted to the equivalent discrete-time model defined by (1) and (2). In the stationary case (where $\mathbf{F}$ is time invariant), or for small sampling intervals Δt, it is well known that

$$\Phi(t_{k+1},t_k) = \Phi(\Delta t) = e^{\Delta t F(t_k)} = \sum_{n=0}^{\infty} \frac{\Delta t^n}{n!} F^n(t_k)$$

$$\text{where} \qquad \Delta t = t_{k+1} - t_k \quad . \tag{27}$$

The product $\Gamma\underline{w}$ in Equation (1) is defined as

$$\Gamma(k)\underline{w}(k) = \int_{t_k}^{t_{k+1}} \Phi(t_{k+1},\tau)G(\tau)\underline{w}(\tau)d\tau \tag{28}$$

and an approximate solution of this integral for small sampling intervals is easily found by substituting the expansion for the Φ matrix. Application of the above approximations yields the following matrices if terms of the order Δt^3 and higher are ignored:

$$\Phi = \begin{bmatrix} 1 - \frac{C}{Re} & 0 & \Delta t(g+\dot{w}_m) & \Delta t & C & 0 \\ \Delta t & 1 & C & \frac{\Delta t^2}{2} & 0 & 0 \\ -\frac{\Delta t}{Re} & 0 & 1 - \frac{C}{Re} & -\frac{\Delta t^2}{2Re} & \Delta t & 0 \\ 0 & 0 & 0 & 1 & 0 & 0 \\ 0 & 0 & 0 & 0 & 1 & 0 \\ 0 & 0 & 0 & 0 & 0 & 1 \end{bmatrix}$$

where $$C = \frac{\Delta t^2(g + \dot{w}_M)}{2} \qquad (29)$$

and

$$\Gamma = \begin{bmatrix} \Delta t & C \\ \frac{\Delta t^2}{2} & 0 \\ -\frac{\Delta t^2}{2Re} & \Delta t \\ 0 & 0 \\ 0 & 0 \\ 0 & 0 \end{bmatrix} \qquad (30)$$

The covariance matrix for the plant noise vector is expressed by a simple diagonal matrix with elements

$$Q(k) = Q = \text{diag}[\sigma^2_{w1}\ 0\ \sigma^2_{w3}\ 0\ 0\ 0\ ] \qquad (31)$$

where σ^2_{wi} is the variance of the noise process. Similarly the covariance matrix (or scalar in this case) for the measurement process is

$$R(k) = R = \sigma^2_{v1} \quad . \qquad (32)$$

In order to initiate the Kalman filter, it is necessary to specify an initial state estimate, $\hat{\underline{x}}(0)$, and its associated *a priori* covariance matrix, P(0). This covariance matrix is simply a diagonal matrix consisting of the variances of the individual initial state error variances. The initial estimate of the state variables in this investigation are assumed to be zero. All terms required by the filter are now defined and the equations in 3.2 can be used to estimate the errors in the measurement signals optimally.

4.0 Results and Discussion

The equations employed in this study for the ground roll simulation of the dynamic model are nominally the set for the Boeing 747 aircraft. Algorithms were also developed to simulate the sensors mounted on the aircraft with all their attendant errors and noise values. The simulations considered below were conducted on an IBM 3090 mainframe with the aid of a dynamic systems simulation package, 'SCSIM', available within the Aerospace Engineering Department of the University of Bristol. These time responses were performed for standard sea level conditions.

The filter algorithms described in 3.2 are greatly simplified as the scalar measurement case is presented here. The appropriate simplifications (eg. matrix inversion avoided) have been made in the implementation.

Fig. 7 below shows the runway position and velocity as measured by the independent measurements alone compared with true values (eg. distance errors growing to over 200 m), whereas Fig. 8 (note change of scales) shows how closely the filter can track the true values when the multiple sources contribute to the hybrid configuration (eg. comparable distance errors growing to about 15 m).

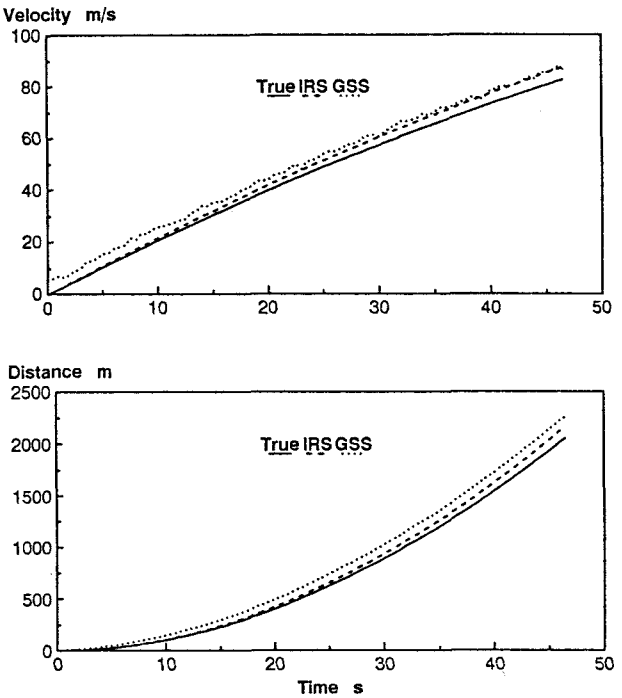

Fig. 7 True and Unfiltered Measurements Signals

These error states are used to correct the IRS outputs and the resulting best estimates are presented to the prediction and display routines. Thus two independent measurements have been combined to eliminate significant errors which are generally evident in each. Optimal estimates of the take-off conditions also enhance the accuracy of the predictive performance routines. Consequently the likelihood of displaying hazardously misleading information is reduced, which ultimately implies greater reliability and improved pilot action. This superior system reliability is crucial in providing positive evidence that both pilots and airworthiness authorities should accept the take-off monitor.

The tilt error and gyroscope drift rate bias have been included in the state model in order to provide a more complete dynamic model of the system and also to illustrate the effectiveness of the filter. These parameters are not required for use outside the filtering algorithms. The relatively small magnitude of these states implies that their contribution to the uncertainties in the acceleration signal is minor. For example, the magnitude of b_α was correctly estimated to fluctuate about 4.8×10^{-7} rad/s (and is therefore not illustrated above). In these situations, simplifications to reduce the order of the state model are appropriate. The resulting state vector could consist of only four states, namely Δu, Δx, b_a and b_g.

The matrices required for the filter implementation would be simplified and in addition the '$(g + \dot{w}_M)$' term would disappear from the **F** matrix. Consequently the computational burden of implementing the Kalman filter is reduced. Fictitious plant noise can be added to combat divergence due to this intentional incorrect plant modelling. The actual level of noise can be determined by a number of techniques which vary from trial and error methods to more complex systematic approaches[6]. Only a comprehensive sensitivity analysis can determine the effectiveness of the reduced order model.

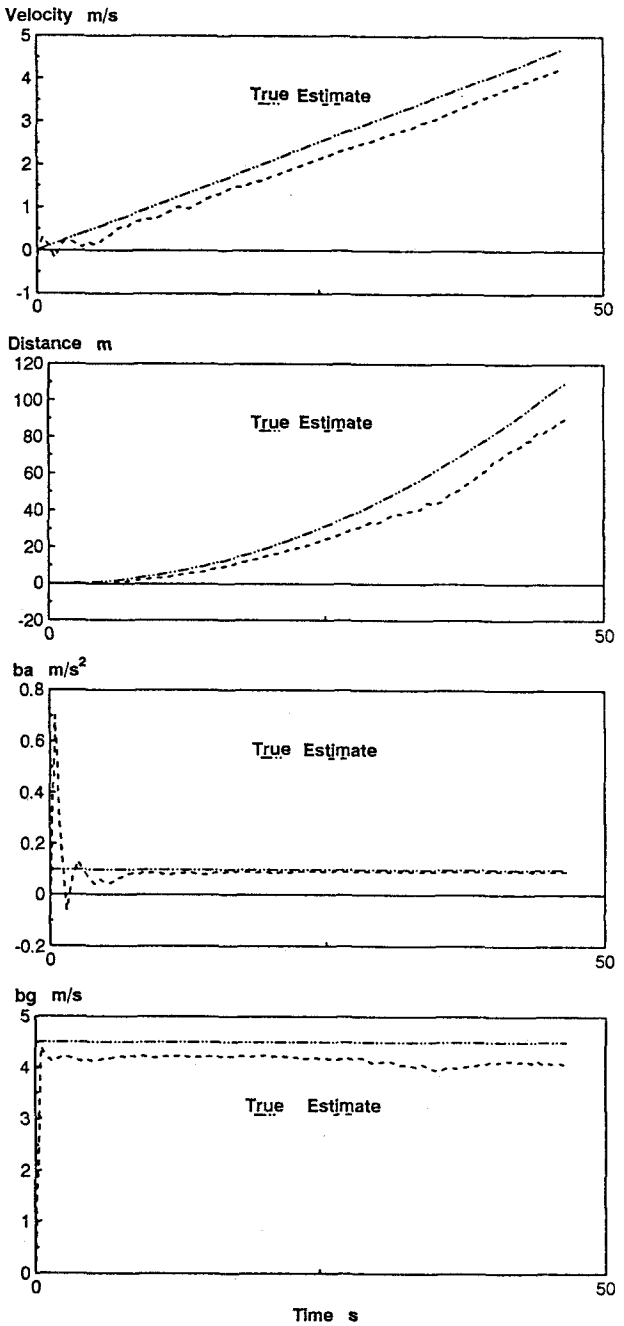

Fig.8 Actual and Estimated Measurement Errors

5.0 Conclusions

The performance being achieved and the approach of a potentially dangerous situation during take-off cannot be observed without special instrument aids. Detection of any shortfall in the performance early in the take-off run would thus not only prevent a high speed overrun, but would aid the pilot in judging the point at which an undisturbed take-off were both possible and safe. The Kalman filter can be employed as a state estimator to deduce optimal estimates of the take-off conditions and consequently enhance the accuracy and reliability of the TOPM. However, the acceptability of the take-off monitor to pilots and airworthiness authorities will require considerable parallel efforts.

6.0 References

[1] SAE. Take-Off Performance Monitor (TOPM) System, Airplane, Minimum Performance Standard for, *Aerospace Standard AS 8044*, 1987.

[2] Ashford R. *Overruns on Landing and Rejected Take-Offs*, Civil Aviation Authority, Redhill, 1984.

[3] Khatwa R. *The Development of a Take-Off Performance Monitor*, PhD Thesis (in preparation), University of Bristol, Department of Aerospace Engineering, 1990.

[4] Khatwa R. Engine Monitors for Efficient Take-Off Performance Monitors, 2nd *International Congress on Condition Monitoring and Diagnostic Engineering Management (COMADEM 90)*, Brunel University, London, 16-18th July 1990.

[5] Srivatsan R. Design of a Take-Off Performance Monitoring System, DE Dissertation, University of Kansas, Department of Aerospace Engineering, 1985; also published as *NASA CR-178255*, 1987.

[6] Jazwinski A H. *Stochastic Processes and Filtering Theory*, Academic Press, New York, 1977.

[7] Kaminski P G, Bryson A E Jr and Schmidt S F. Discrete Square Root Filtering: A Survey of Current Techniques, *IEEE Trans on Automatic Control*, Vol AC-16, No 6, 1971, pp.727-736.

[8] Andrews A. A Square Root Formulation of the Kalman Covariance Equations, *AIAA Journal*, Vol. 6, No. 6, 1968, pp. 1165-1166.

7.0 Acknowledgements

The work reported herein was supported by the UK Science and Engineering Research Council. The author wishes to record his debt to Dr. D L Birdsall and Dr. D A Cowling for supervision of this project. In addition, thanks are due to Dr. R Stirling for use of the systems simulation package 'SCSIM'.